THE JOURNAL OF PHYSICAL CHEMISTRY B

Article

pubs.acs.org/JPCB

Designing Nanoparticle Translocation through Cell Membranes by Varying Amphiphilic Polymer Coatings

Liuyang Zhang, Matthew Becton, and Xianqiao Wang*

College of Engineering and NanoSEC, University of Georgia, Athens, Georgia 30602, United States

ABSTRACT: Nanoparticle (NP)-assisted drug delivery has been emerging as an active research area. Understanding and controlling the interaction of the coated NPs with cell membranes is key to the development of the efficient drug delivery technologies and to the management of nanoparticle-related health and safety issues. Cellular uptake of nanoparticles coated with mixed hydrophilic/hydrophobic polymer ligands is known to be strongly influenced by the polymer pattern on the NP surface and remains open for further exploration. To unravel the physical mechanism behind this intriguing phenomenon, here we perform dissipative particle dynamics simulations to analyze the forces and efficacy time as the copolymer-coated NPs pass through the lipid bilayer so as to provide better design of coated NPs for future drug delivery applications. Four characteristic copolymer ligands are constructed to perform the simulations: hydrophilic−hydrophobic (AB), hydrophobic−hydrophilic (BA), hydrophobic−hydrophilic−hydrophobic−hydrophilic (BABA), and a random pattern with hydrophilic and hydrophobic beads. We mainly study the critical force and potential of mean force required for entering inside of the lipid bilayer and penetration force to pass all the way through the cell membrane as well as the translocation time for these patterned NPs across the bilayer. Through copolymer ligand pattern designing, we find a suitable nanoparticle candidate with a specific polymer coating pattern for drug delivery. These findings provide useful guidelines for the molecular design of patterned NPs for controllable cell penetrability and help establish qualitative rules for the organization and optimization of copolymer ligands for desired drug delivery.

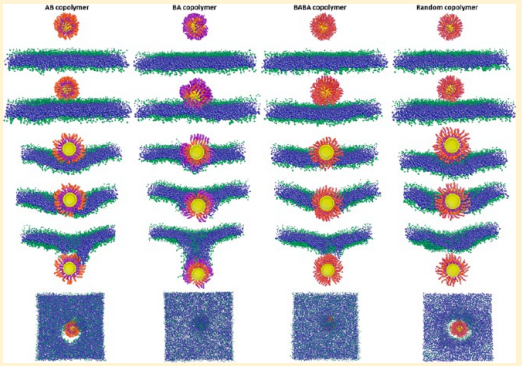

INTRODUCTION

Recent years have witnessed the explosive growth of interest in nanoparticles (NPs) with a wealth of biomedical applications because they are widely used as carriers to translocate drug molecules and useful materials into cell interiors. For these applications, the efficient uptake of NPs into cells emerges as a critical issue by requiring the capability of NPs to transport through cell membranes while NPs adhering to cells may trigger damage to the cell membrane and induce adverse biological effects with the potential to introduce cytotoxicity.[1−3] With this regard in mind, understanding the fundamental mechanism of cellular uptake of NPs holds the key to the advancement of NP biomedical applications.

Due to the extremely small size, high surface energy, and high surface area of the NP, the interaction between cells and NPs can be heavily influenced by intelligent surface structure design.[4,5] It has been realized that functionalized gold NPs can potentially deliver nucleic acids into the cell.[6] Peptide-functionalized NPs have been identified as an efficient homing device to selectively target pancreatic cancer cells,[7] while folic-acid-functionalized NPs can enhance the oral absorption of drugs with poor oral bioavailability.[8] Typically, NP interactions with cell membranes are dictated by the chemical functionalities of the surface coating in addition to their shape, size, and relative arrangement.[9−12] A variety of polymers have been demonstrated to generate chemically nanopatterned NPs and modulate their stimuli-responsiveness as well as to direct their assembly into hierarchically organized superstructures.[13−16] Amphiphilic copolymers can form micellar structures with a hydrophobic core when in hydrophilic solvent.[17] The amphiphilic polymer hybrid NP consisting of three distinct functional components of a hydrophobic polymeric core, hydrophilic polymeric shell, and lipid monolayer behaves as a robust drug delivery platform with high drug encapsulation yield and tunable and sustained drug release profile.[18−21] However, the design principles of synthetic nanoscaffolds with amphiphilic polymers for membrane transport are far from being comprehensively understood. The shell formed by the polymer can protect the core by decreasing the contact with inactivating species in the aqueous phase. When the coating interacts with biocomponents such as cells and proteins, it affects their pharmacokinetics and disposition as well as their surface properties. Here, we propose four different kinds of copolymer ligands to investigate the impact of surface properties with respect to grafting pattern, density, and rigidity of the polymer on the NP surface. The copolymer ligands are considered to be linear and composed of different patterns of hydrophobic and hydrophilic beads.

Meanwhile, understanding the mechanical properties and damage-response characteristics of biological cells caused by NP translocation is essential for effective therapeutic and scientific

Received: January 26, 2015
Revised: February 11, 2015
Published: February 12, 2015

DOI: 10.1021/acs.jpcb.5b00825
J. Phys. Chem. B 2015, 119, 3786−3794

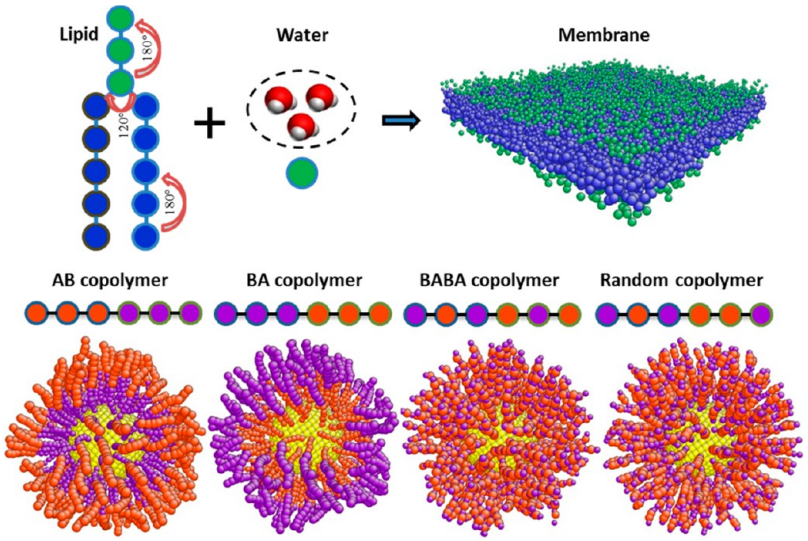

Figure 1. Schematic representation of the DPD model. In the following figures, unless otherwise stated, the hydrophobic bead on the membrane is shown in blue while the hydrophilic is shown in green. To distinguish from the cell membrane, NP is shown in yellow, the hydrophobic bead of the copolymer ligand is shown in purple, while the hydrophilic bead is shown in brown. The number of beads in a ligand is fixed as 12.

application in the medical field, but the 4−6 nm thick plasma membrane presents a challenging barrier that prevents it from accessing the cytosol.[22,23] Particularly, the effect of externally applied force on internal cells should be assessed in order to design robotic surgical tools with optimal force during surgical operations at nanoscale resolution.[24−28] In this paper, by using a dissipative particle dynamics (DPD) method, we will assess various types of forces that affect the passage of the hybrid NPs across the cell membrane. The information about the forces experienced is important for individual cell-based diagnosis and pharmaceutical applications.

MODEL AND METHOD

The simulations in this paper are based on DPD, a mesoscopic coarse-grained simulation method for soft materials and biomembrane systems.[29,30] In DPD simulation, a small group of atoms is treated as a single bead located at the center of mass of the group. Beads i and j interact with each other via a pairwise force consisting of a conservative force F_{ij}^{C} representing thr excluded volume effect, a dissipative force F_{ij}^{D} representing viscous drag between moving beads, and a random force F_{ij}^{R} representing stochastic impulse. Both F_{ij}^{D} and F_{ij}^{R} act together as a thermostat for the beads. Similar to molecular dynamics simulation, time evolution is also governed by the Newton's equation of motion. The total force on bead i can be expressed as

$$F_i = \sum_{i\neq j} (F_{ij}^{C} + F_{ij}^{D} + F_{ij}^{R})$$
$$= \sum_{i\neq j} (a_{ij}\omega(r_{ij})\hat{r}_{ij} - \gamma\omega^2(r_{ij})(\hat{r}_{ij}\cdot v_{ij})\hat{r}_{ij} + \sigma\omega(r_{ij})\zeta_{ij}\Delta t^{-1/2}\hat{r}_{ij})$$

where a_{ij} is the maximum repulsive force, r_{ij} the distance, $\hat{r}_{ij}$ the unit vector, and v_{ij} the relative velocity between beads i and j; ζ_{ij} denotes a random number with a zero mean and unit variance, and

$$\omega(r_{ij}) = \begin{cases} 1 - \dfrac{r_{ij}}{r_c} & r_{ij} < r_c \\ 0 & r_{ij} > r_c \end{cases}$$

is a normalized distribution function, with r_c being the cutoff radius. The parameters γ and σ are related to each other as $\sigma^2 = 2\gamma k_B T$, with $k_B T$ being the unit of energy. The standard values $\sigma = 3.0$ and $\gamma = 4.5$ are used in our study.[9] The mass, length, and time scales are all normalized in the DPD simulations; the unit of length is taken to be the cutoff radius r_c, the unit of mass is that of the solvent beads, and the unit of energy is $k_B T$, as previously stated. All other quantities are expressed in terms of these basic units. The reduced DPD units can be converted to SI units by examining the membrane thickness and the lipid diffusion coefficient. The simulated value of the bilayer thickness is $5r_c$, and the effective time scale of the simulation can be determined from the simulated lateral diffusion constants of the lipid bilayer.[31] The DPD bilayer thickness is about 4 nm, with a diffusion coefficient of around 5 $\mu m^2\ s^{-1}$;[32] by comparison with typical experimental values, it can be shown that one DPD length unit corresponds to approximately 0.8 nm in physical units and the time unit to $\tau = 24.32$ ps. The time step is taken as $\Delta t = 0.01\tau$. All simulations are performed using LAMMPS.[33]

The dimension of the simulation box is $30r_c \times 30r_c \times 50r_c$. The system contains a total of 135 208 particles, composed of 118 603 solvent (water) beads and 16 605 hydrophobic\hydrophilic beads (992 lipid molecules for the bilayer membrane, 512 hydrophobic bead for the rigid spherical NP of diameter 3.6 nm coated with a selected pattern of hydrophilic−hydrophobic copolymer ligand), with a particle density of approximately 3.[34] The solvent beads are not shown in the following plots for clarity. The lipid molecule is represented by the coarse-grained model proposed by Groot and Rabone,[29] as shown in Figure 1, with 3 lipid hydrophilic head beads and 10 lipid hydrophobic tail beads. On the basis of the arrangement of the hydrophilic and hydrophobic beads along the chain, four patterns of copolymer ligand are classified as AB, BA, BABA, and random pattern, as seen in Figure 1. The hydrophilic beads and hydrophobic beads are shown as green and blue, respectively. The repulsive interaction parameter between the same type of beads within the NP, copolymer ligands, and membrane is set as $a_{ij} = 25$, and for two beads of different types, it is set as $a_{ij} = 100$. Within a lipid molecule and copolymer ligand, there is also an elastic harmonic force

DOI: 10.1021/acs.jpcb.5b00825
J. Phys. Chem. B 2015, 119, 3786−3794

$$F_{ij}^{S} = k_s\left(1 - \frac{r_{ij}}{r_s}\right)\hat{r}_{ij}$$

used to connect two consecutive beads, where k_s and r_s are the spring constant and equilibrium bond length, respectively. Here, we use $k_s = 100.0$, $r_s = 0.7r_c$ for the lipid molecule[35] and $k_s = 200.0$, $r_s = 0.25$ for the copolymer ligand.[9] The copolymer ligands are also anchored to the NP surface by a spring force $k_s = 200.0$, $r_s = 0.25$ in order to prevent the rearrangement or detachment of the coating copolymer ligands during the simulation. The bending resistance of the lipid and copolymer chain is represented as an additional force due to a harmonic constraint on two consecutive bonds

$$F^{\theta} = -\nabla V_{\text{bend}} = -\nabla[k_\theta(\theta - \theta_0)^2]$$

where k_θ, θ, and θ_0 are the bending constant, inclination angle, and equilibrium angle, respectively. For three consecutive lipid tail beads or three consecutive lipid head beads in a lipid molecule, we take $k_\theta = 6$ and $\theta = 180°$; for the last head bead and the top 2 tail beads, $k_\theta = 3$ and $\theta = 120°$; for the bottom two consecutive head beads and the first bead in each tail, $k_\theta = 4.5$ and $\theta = 120°$.[9] For three consecutive copolymer ligand beads, we take $k_\theta = 5$ and $\theta = 180°$.

RESULTS AND DISCUSSIONS

For a pure hydrophobic NP, it is very challenging for it to enter inside of a cell membrane as the hydrophobic lipid tails of the NP

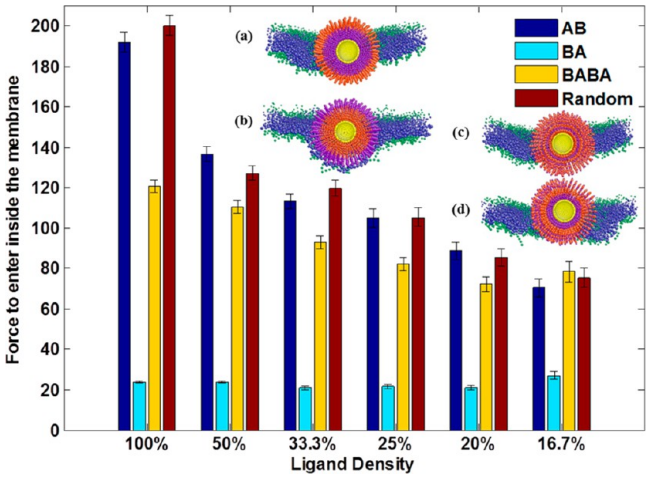

Figure 2. Evolution of the entry force with the ligand coating pattern and density. Subplots (a–d) show the entry moment of AB, BA, BABA, and random patterned NP, respectively.

inhibit its further penetration after it attaches to the membrane surface. However, different ligands outside of the NP could change its chemical properties and manipulate the penetration process. To initiate the penetration process, the patterned NP needs to overcome the mandatory energy barrier in order to go inside of the cell membrane. With a coating of copolymer ligands, it should be interesting to study how large of a force is needed for the coated NP to enter inside of the cell membrane. The patterned NP is initially placed a distance of $15r_c$ away from the membrane in the z direction. The system is relaxed for 12.16 ns while the NP is fixed. The edges of the lipid bilayer are then fixed, and the NP is pulled down toward the bilayer membrane by using steered molecular dynamics (SMD) with a constant pulling

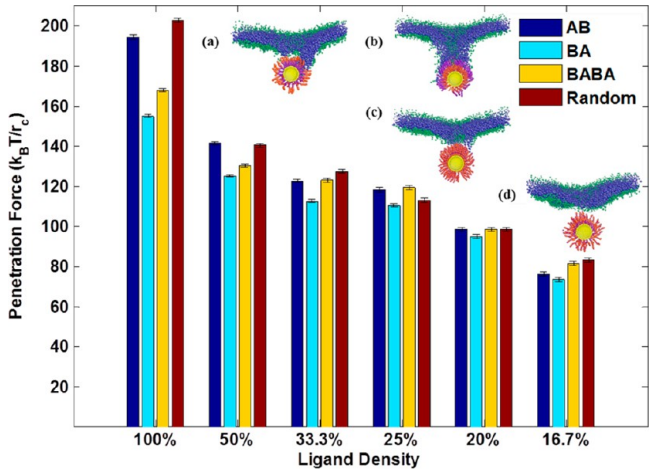

Figure 3. Evolution of the penetration force with the ligand coating pattern and density. Subplots (a–d) show the penetration through the moment of AB, BA, BABA, and random patterned NP, respectively.

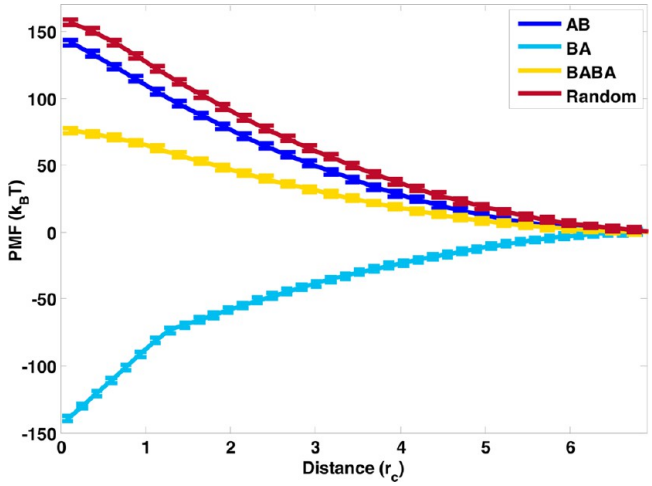

Figure 4. The PMF as a function of the distance between the NP and the bilayer membrane center under different coating patterns of the NP. The coating density is set as 100%.

velocity of $0.1r_c/\tau$.[36] Here, we systematically study the entry force F_E for different copolymer patterns at different coating densities ρ (100, 50, 33.3. 25, 20, 16.7%), as shown in Figure 2. F_E is calculated by averaging the force when the NP attaches to the membrane surface and the force when the NP arrives in the middle of the bilayer. For the AB and random patterns, the NP cannot enter inside of the membrane easily due to the energy barrier caused by the central hydrophobic layer of the membrane. As the driving force continues to increase, the membrane begins to bend until it fractures at an $F_E = 191.9k_BT/r_c$. For the BA pattern, because the outer hydrophobic property of the copolymer pattern makes it less inclined to stay in the hydrophilic environment (water), the NP takes less effort to attain entry into the membrane with an average $F_E = 23.04k_BT/r_c$. The F_E shows little difference between different coating densities, which further demonstrates that spontaneous entry of a NP is likely to occur for the BA pattern when it approaches the membrane[11] Similar to the AB pattern, the F_E for the BABA pattern decreases with the coating density; however, the NP can get inside of the membrane more easily. It is also observed that when the coating density is lowered to ρ = 16.7%, the

DOI: 10.1021/acs.jpcb.5b00825
J. Phys. Chem. B 2015, 119, 3786–3794

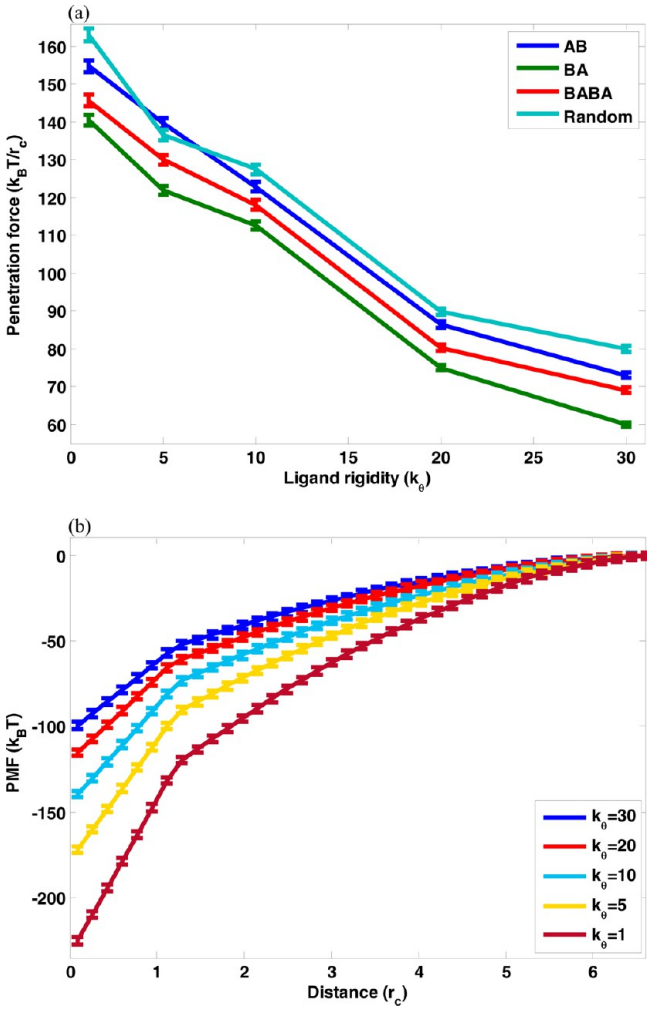

Figure 5. (a) Penetration force as a function of ligand rigidity of different coating patterns. (b) PMF as a function of the distance between the NP with the BA coating pattern and the bilayer membrane center under different bending rigidity of the coating polymer. The coating pattern is BA, and the coating density is chosen as 100%.

hydrophobicity of the pure NP appears to contribute to an increment of the entry force compared with a high-density coating. For the BABA pattern, F_E increases from $72.36k_BT/r_c$ to $78.41k_BT/r_c$, while for the BA pattern, F_E increases from $21.1k_BT/r_c$ to $27.1k_BT/r_c$. For the AB and random patterns, the outside hydrophobic portion of the copolymer ligand possesses similar properties as the naked NP; therefore, F_E is consistent with the abatement of ligand density. According to Figures 2 and 3, the critical forces for the NP to enter and penetrate decrease with decreasing grafting density. It seems that a bare NP (without surface coating) could be more efficiently uptaken by the cell. However, interactions of a NP with the cell membrane are dictated by the chemical properties of the surface coating of the NP in addition to its shape, size, and relative arrangement. The NP with an amphiphilic polymer consisting of three distinct functional components, a hydrophobic polymeric core, hydrophilic polymeric shell, and lipid monolayer, behaves as a robust drug delivery platform with high drug encapsulation yield and a tunable and sustained drug release profile. For a pure hydrophobic NP, it is very challenging for it to enter inside of a cell membrane as the hydrophobic lipid tails of the NP inhibit its further penetration after it adheres to the membrane surface. However, NPs with different grafted ligands could change its chemical properties and manipulate the penetration process due to external stimuli such as pH and temperature. Besides, the pure NP may trigger damage to the cell membrane and introduce nanotoxicity. These aforementioned points illustrate the advantage of the grafted NPs.

To further explain the effect of copolymer ligand patterns of NPs on their penetrability into cells, here we investigate the penetration force F_P for different hybrid NPs. At the beginning of the NP translocation process, in order to penetrate through the first layer of the lipid membrane, the NP needs to push the first layer and tear the head groups apart to make room for its penetration. The resistance from the head group depends on the ligand types on the NP surface.[37] This explains why F_E is needed to enter inside of the lipid bilayers. However, different from F_E, F_P is defined as the value of the pulling force when the NP detaches from the membrane after passing through. When the NP crosses the second layer, the attractive interaction between lipid tails and the NP slows down the movement of the NP. F_P should be large enough for the NP to exit the cell membrane. As shown in Figure 3, F_P displays a similar downtrend to F_E for decreasing density of the ligand coating. Interestingly, the AB and random patterns do not show any difference for F_E and F_P due to density. The AB and random patterned NPs leave the membrane quickly after entering inside as the membrane structure is broken after accumulative bending. F_P varies from $195k_BT/r_c$ to $80k_BT/r_c$ as coating densities decrease, which is in good agreement with previous research work.[9,10] For the AB pattern, the hydrophilic outlayer of the coating copolymer on the shell prohibits the NP from entering inside of the middle hydrophobic layer of the bilayer membrane. However, when it enters inside of the lipid bilayer, the hydrophilic outlayer coating of the NP makes it easy to get out of the hydrophobic middle layer of the membrane. This also explains why the force to enter inside of the membrane is different from the force penetration through the membrane. However, for the BA pattern, penetration is impeded by the middle hydrophobic layer of the membrane, which leads to a large difference between the entry force $F_E = 23.8k_BT/r_c$ and the penetration force $F_P = 155.2k_BT/r_c$ at $\rho = 100\%$. There exists a large friction between the BA pattern NP and the membrane during the final stages of translocation. The BABA pattern also shows differences between $F_E = 120.7k_BT/r_c$ and $F_P = 167.9k_BT/r_c$ due to its layer-by-layer arrangement of hydrophilic and hydrophobic beads. The frictional effect however is not as obvious compared to that of the BA pattern. In order to obtain a more quantitative picture of the interaction between patterned NPs and the bilayer membrane, we take patterned NPs with 100% coating density as an example to calculate the potential of mean force (PMF) as shown in Figure 4. The PMF has been considered an important factor to understand the penetration process of the NP through the cell membrane. According to data analysis, for the BA pattern, the free energy decreases as the NP enters the bilayer membrane, indicating that there is a preferred location inside of the membrane for the BA pattern. For AB, BABA, and random patterns, the free energy increases as the NP enters inside of the lipid bilayer. Due to the symmetric structure of the bilayer membrane and the NP, the BA patterned NP can easily enter inside of the membrane; however, it is difficult for it to get out of the membrane. It is relatively easy for the BABA patterned NP to enter inside of the membrane conpared to the AB and random patterned NP. The free-energy change corresponding to the phenomena that we observed for different

DOI: 10.1021/acs.jpcb.5b00825
J. Phys. Chem. B 2015, 119, 3786−3794

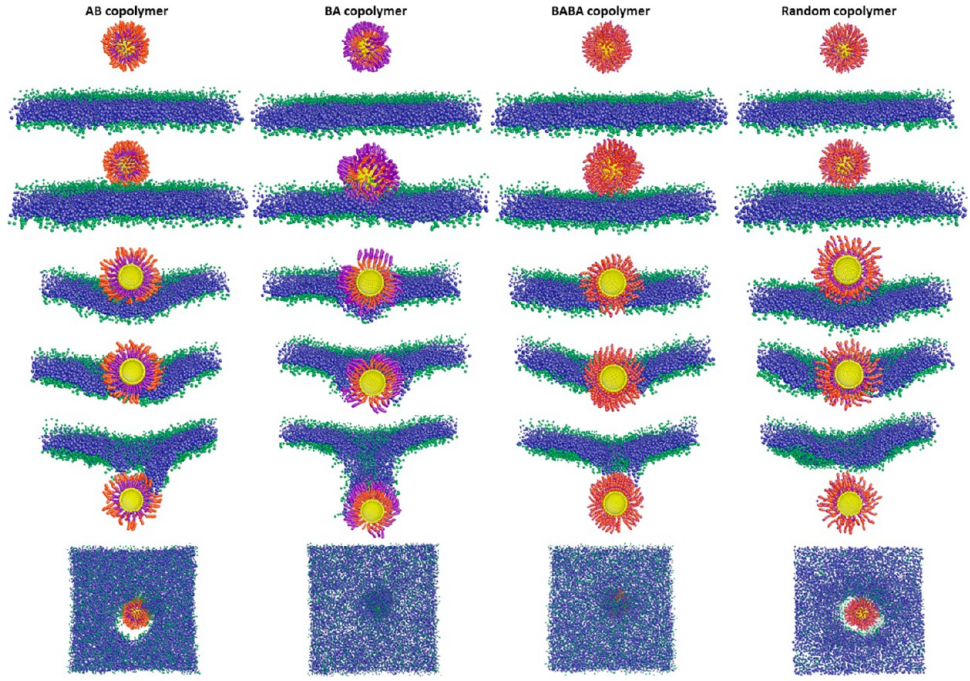

Figure 6. Dynamic process of four different patterned NPs passing through the cell membrane.

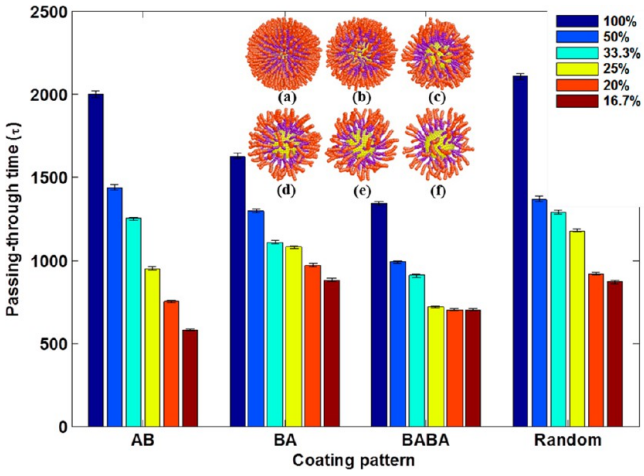

Figure 7. Translocation time as a function coating pattern and coating density. Subplots (a–f) show the different densities of the AB patterned NP.

patterned NPs is in good agreement with that of other researchers' work.[9,38]

Actually, the NP can be either rigid or soft depending on the ligand coating. Here, the conformational characteristics of the ligand consisting of a flexible backbone depend on the rigidity of the chain that is simply described by k_θ, the angle potential constant between the ligand beads. The angle potential confines the freedom degree of the ligands. Because the extendibility of the ligands is constrained by the rigidity, the ligands are approximately distributed uniformly on the surface when k_θ increases. As shown in Figure 5a, despite coating ligand patterns, F_P decreases with the increase of rigidity, causing the more rigid NPs to create small deformations in the membrane so that it is easier for them to pass through despite their hydrophobicity, which is in agreement with high rigidity leading to a high engulfment degree of NPs.[12] To better quantify the effect of bending rigidity of coated polymers on the penetration process of NPs, we take the BA patterned NP as an example to depict the free-energy change described by the PMF. In Figure 5b, as the bending rigidity increases, the change of the PMF decreases, which means that the critical force for NPs to penetrate the lipid bilayer decreases. A possible explanation is that as the bending rigidity of the coating polymer increases, the polymer loses certain flexibility to accommodate its configuration change, therefore lowering the adhesive interaction between coating polymers and the cell membrane.

Figure 6 shows the whole penetration process for the AB, BA, BABA, and random patterns. For the purpose of illustration, the coating density is chosen as 33.3%. The whole penetration process is comprised of three phases: attaching, inserting, and detaching. For the AB pattern, the hydrophilic outside layer of the NP closely attaches to the hydrophilic lipid head on the membrane; however, it cannot get through the hydrophobic layer composed of lipid tails. For the BA pattern, the NP is difficult to attach to the cell membrane surface without any external force; however, it can easily enter inside of the hydrophobic layer of the membrane after attaching the membrane surface. The alternate hydrophobic–hydrophilic behavior of the NP with the BABA pattern attenuates the interaction between the NP and membrane when the NP attaches to and passes through the cell membrane. The NP passing the membrane can introduce disruption of the cell membrane and may cause cell death.[4,39−42] From the penetration process, it can be found that the cell membrane is strongly affected by different ligand coatings on the NP. The AB pattern and random pattern leave a hole on the membrane when they pass through the cell membrane, which breaks the integrity of the cell membrane. The BA patterned NP does not bend the membrane to such an extent before entry; however, it prefers to stay with the hydrophobic lipid tails when pulled out. The mild deformation of the membrane is quickly healed by the hydrophobic lipid tails refilling the hole created by the BA patterned NP. A portion of lipid tail is pulled out as well with the NP, which indicates strong friction between the NP and the

DOI: 10.1021/acs.jpcb.5b00825
J. Phys. Chem. B 2015, 119, 3786−3794

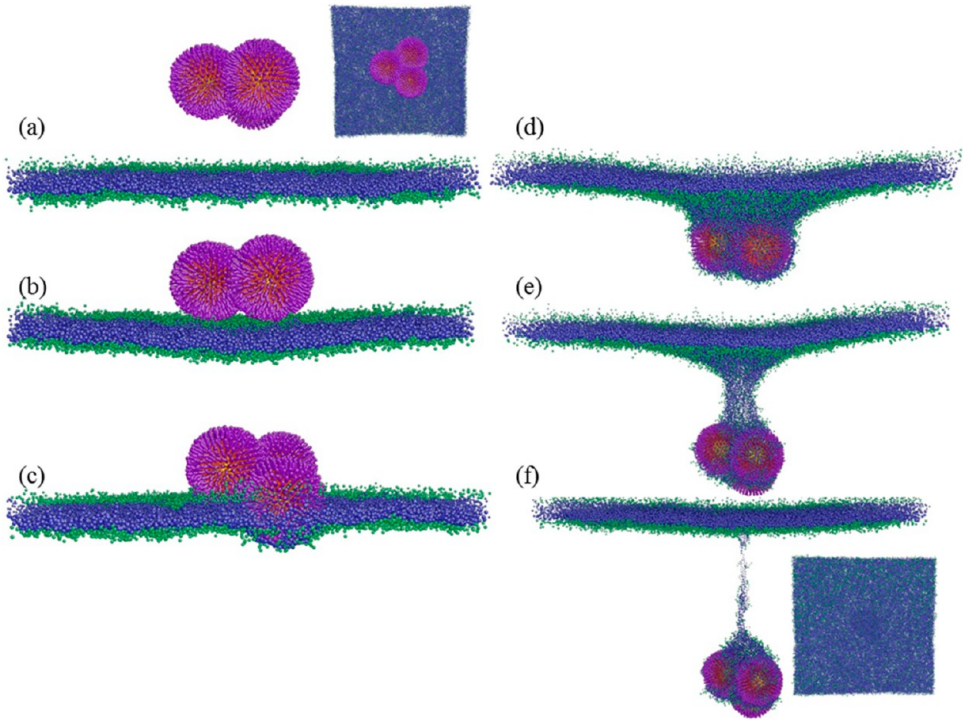

Figure 8. Dynamic process of a group of BA patterned NPs passing through the membrane with the highest coating density (100%).

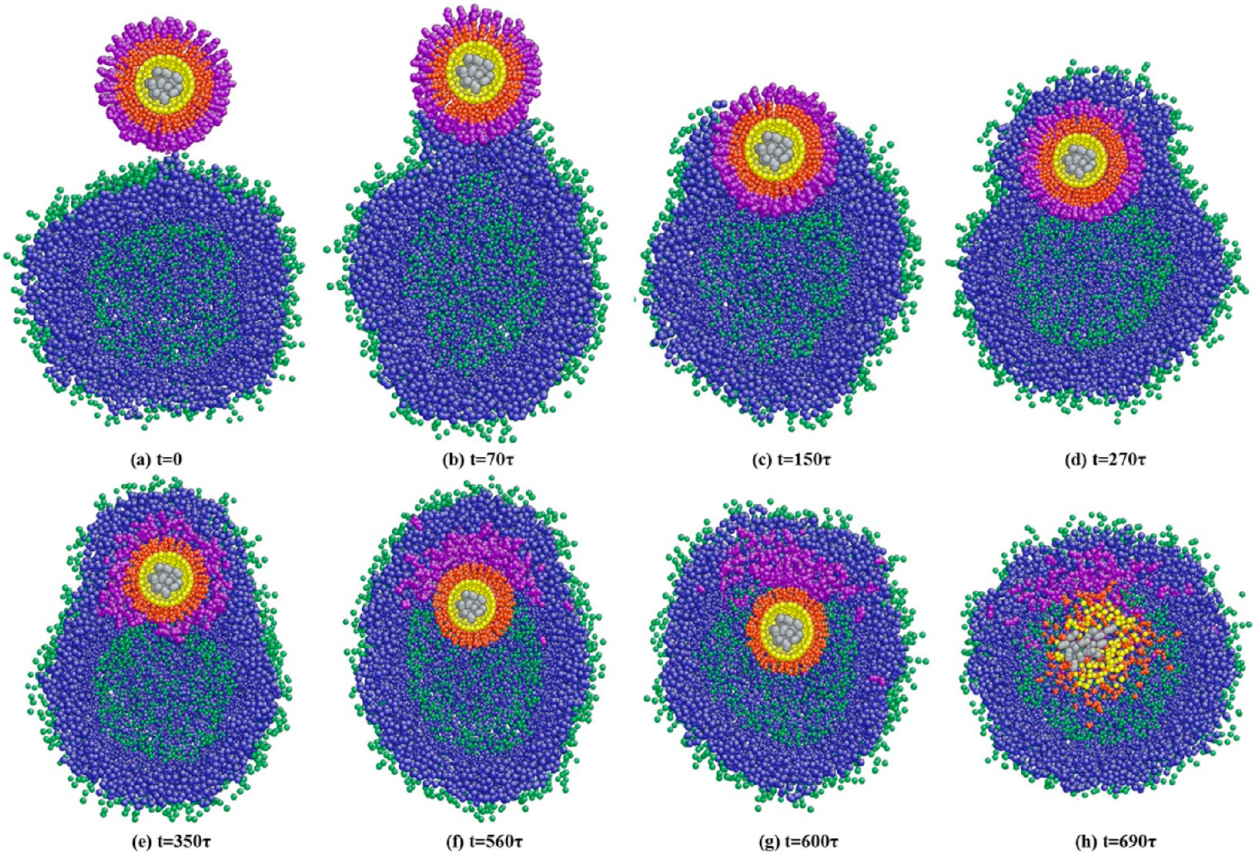

Figure 9. Dynamic process of the drug delivery based on the BA patterned NP. The drug particle is shown in gray color.

membrane. For the BABA pattern, the NP does not break the membrane by creation of a hole accompanied by a few lipid molecules leaving from the cell membrane system. These intriguing findings inform us that the BA and BABA patterns are robust coating strategies for the NP as they do not cause permanent damage to the cell membrane when penetrating it. Understanding the penetration force is helpful to design healthy and robust drug delivery nanodevices.

DOI: 10.1021/acs.jpcb.5b00825
J. Phys. Chem. B 2015, 119, 3786−3794

The translocation time, the time that a particle passes through the cell membrane, is a key factor for a cell to regulate the movement of a variety of substances in order to maintain the functional balance of ions, water, oxygen, carbon dioxide, nutrients, and other molecules.[43] Understanding the translocation time for a NP to enter inside of the cell is crucial to the bioactivities necessary for maintaining the function of the cell and drug delivery system. The translocation time of the drug through the cell membrane is also crucial for drug delivery efficiency.[11] By tuning the coating pattern, density, and rigidity of the polymer on the surface of the NP, we can control the drug delivery process. Therefore, the translocation time of the NP through the cell membrane is an important factor for evaluating the drug delivery efficiency. Here, we investigate the translocation time for the patterned NP with different ligands, as shown in Figure 7. The translocation time is defined as time difference between when the NP attaches to the membrane surface and when it leaves the opposite side of the membrane. For all types of patterns, the translocation time is shortened with a decrease of ligand density. At high density, the BABA patterned NP needs the shortest time to pass through the membrane because it overcomes a smaller energy barrier than the AB pattern and does not have as large of a friction inside of the membrane as the BA pattern. The BA patterned NP is challenging to move out from the hydrophobic middle layer, as we discussed in the previous section; therefore, it takes a relatively long time to pass through the membrane. The AB and random patterns take a longer time to pass through the membrane at high density because of the difficulty in entering the membrane. From the analysis of the translocation time, the coating pattern plays a crucial role in designing the NP complex, and the BABA pattern is the most efficient and preferable coating to allow a NP to pass through the membrane easily.

NPs are known to have high drug-loading capacity, high water solubility, and appropriate size for long circulation in the blood. The core−shell architecture of hybrid NPs possesses advantages for drug delivery with their unique core−shell architecture. The hydrophobic drugs can be solubilized into the hydrophobic core by interactions such as metal−ligand coordination bonding and electrostatic interaction.[44−46] From the discussion of the four coating patterns above, the BA pattern is chosen to design a drug delivery carrier as it needs the least energy to enter inside of the cell. However, the BA pattern has difficultly leaving the membrane and getting inside of the cell. Also, as expected, the BA patterned NPs can conglomerate together in the solvent if they get exposed together. However, in Figure 8, we have demonstrated that agglomerated NPs can be considered as a large hydrophobic particle, and it still can enter inside of the cell by a similar mechanism as we discussed for a single BA patterned NP in Figure 6. The membrane keeps its integrity except for that a portion of lipids are carried away with the large BA patterned NP. For an ideal drug delivery vector, in addition to the NPs' entry inside of the cell membrane, the outside hydrophobic layer of the NP needs to be detached from the NP in order to get into the cell when the hybrid NP enters inside of the membrane. The detaching process can be done by creating dynamic covalent bonds between the hydrophobic and hydrophilic portions of the BA copolymer as well as between the NP and copolymer.[11] The dynamic bonds are defined as any class of bond that can selectively undergo reversible breaking and re-formation, usually under equilibrium conditions.[47] The breakage of dynamic covalent bonds can be mimicked by using a pH-sensitive polymer or thermosensitive polymer as the ligand to control the cellular attaching and detaching under different external environments.[48−50] Figure 9 shows the automatic and dynamic process for the BA pattern entering inside of the cell. The BA patterned NP is put $15r_c$ away from the cell. It takes 12 ns before the NP attaches to the cell surface. After attaching, because the surface of the BA pattern is hydrophobic, it can spontaneously insert into the cell membrane, as shown in Figure 9a−d. The internal dynamic bonds of the BA polymer are completely broken in Figure 9e, and the broken polymer branches accumulate behind the NP and slowly diffuse into the middle of the cell membrane. When the bond is broken, the local density of the hydrophobic portion of the BA copolymer prohibits the NP from leaving the cell membrane; therefore, the NP with the remaining hydrophilic covering has more than a 50% probability to enter inside of the cell due to the fact that the hydrophilic portion will prefer not to stay inside of the hydrophobic middle layer. The hydrophilic portion of the BA polymer is dissembled by detaching the bonds through the controllable external stimuli such as pH, light, and temperature, and the drug inside of the core can be released. The method of the drug delivery process that we propose here is considered as a pathway to transport the drug by using multiple shell layers through designing the hydrophobicity of layers. Our simulation offers a novel way to guide nanocarrier design with nanomaterials in medical research.

SUMMARY

In summary, we have performed dissipative dynamics simulation to investigate how the NP coated with different amphiphilic copolymers enters inside of the cell. The entry force and penetration force needed for entry inside of the lipid bilayer and penetration through the cell membrane have been discussed with four different coated NPs. BA and BABA patterns have significant impacts on entry and penetration forces, while the AB and random pattern have negligible effect. Through investigation of the effect of coating density and polymer rigidity for the penetration forces and translocation time, we find that NPs coated with more rigid copolymer ligands possess better capability and use less time to pass through the cell membrane. Our simulation suggests that the NP with copolymer coat can act as a multishell carrier for the desired drug delivery carrier and also provides a design guideline for a novel drug delivery system. Here, we focus on the effect of surface coating of the NP on its entry and penetration forces; there is plenty of room for further exploration on the effect of the NP from its size, shape, and electrical charges.

AUTHOR INFORMATION

Corresponding Author

*E-mail: xqwang@uga.edu. Tel: 706-5426251.

Notes

The authors declare no competing financial interest.

ACKNOWLEDGMENTS

The authors acknowledge support from the University of Georgia (UGA) start-up fund. The facility support for modeling and simulations from the UGA Advanced Computing Resource Center are greatly appreciated.

REFERENCES

(1) Zuzana, M.; Alessandra, R.; Lise, F.; Maria, D. Safety Assessment of Nanoparticles Cytotoxicity and Genotoxicity of Metal Nanoparticles In Vitro. *J. Biomed. Nanotechnol.* **2011**, *7*, 20−21.

(2) Lewinski, N.; Colvin, V.; Drezek, R. Cytotoxicity of Nanoparticles. *Small* **2008**, *4*, 26−49.

DOI: 10.1021/acs.jpcb.5b00825
J. Phys. Chem. B 2015, 119, 3786−3794

(3) Buzea, C.; Pacheco, I. I.; Robbie, K. Nanomaterials and Nanoparticles: Sources and Toxicity. *Biointerphases* **2007**, *2*, MR17−71.
(4) Verma, A.; Uzun, O.; Hu, Y.; Hu, Y.; Han, H.-S.; Watson, N.; Chen, S.; Irvine, D. J.; Stellacci, F. Surface-Structure-Regulated Cell-Membrane Penetration by Monolayer-Protected Nanoparticles. *Nat. Mater.* **2008**, *7*, 588−595.
(5) Nel, A. E.; Madler, L.; Velegol, D.; Xia, T.; Hoek, E. M. V.; Somasundaran, P.; Klaessig, F.; Castranova, V.; Thompson, M. Understanding Biophysicochemical Interactions at the Nano−Bio Interface. *Nat. Mater.* **2009**, *8*, 543−557.
(6) Ding, Y.; Jiang, Z.; Saha, K.; Kim, C. S.; Kim, S. T.; Landis, R. F.; Rotello, V. M. Gold Nanoparticles for Nucleic Acid Delivery. *Mol. Ther.* **2014**, *22*, 1075−1083.
(7) Valetti, S.; Maione, F.; Mura, S.; Stella, B.; Desmaële, D.; Noiray, M.; Vergnaud, J.; Vauthier, C.; Cattel, L.; Giraudo, E.; Couvreur, P. Peptide-Functionalized Nanoparticles for Selective Targeting of Pancreatic Tumor. *J. Controlled Release* **2014**, *192*, 29−39.
(8) Roger, E.; Kalscheuer, S.; Kirtane, A.; Guru, B. R.; Grill, A. E.; Whittum-Hudson, J.; Panyam, J. Folic Acid Functionalized Nanoparticles for Enhanced Oral Drug Delivery. *Mol. Pharmaceutics* **2012**, *9*, 2103−2110.
(9) Li, Y.; Li, X.; Li, Z.; Gao, H. Surface-Structure-Regulated Penetration of Nanoparticles Across a Cell Membrane. *Nanoscale* **2012**, *4*, 3768−3775.
(10) Yang, K.; Ma, Y.-Q. Computer Simulation of the Translocation of Nanoparticles with Different Shapes across a Lipid Bilayer. *Nat. Nanotechnol.* **2010**, *5*, 579−583.
(11) Ding, H. M.; Tian, W. D.; Ma, Y. Q. Designing Nanoparticle Translocation through Membranes by Computer Simulations. *ACS Nano* **2012**, *6*, 1230−1238.
(12) Ding, H. M.; Ma, Y. Q. Role of Physicochemical Properties of Coating Ligands in Receptor-Mediated Endocytosis of Nanoparticles. *Biomaterials* **2012**, *33*, 5798−5802.
(13) Chen, L.; Klok, H. A. "Multifaceted" Polymer Coated, Gold Nanoparticles. *Soft Matter* **2013**, *9*, 10678−10688.
(14) Mout, R.; Moyano, D. F.; Rana, S.; Rotello, V. M. Surface Functionalization of Nanoparticles for Nanomedicine. *Chem. Soc. Rev.* **2012**, *41*, 2539−2544.
(15) Zhang, F.; Lees, E.; Amin, F.; Rivera-Gil, P.; Yang, F.; Mulvaney, P.; Parak, W. J. Polymer-Coated Nanoparticles: A Universal Tool for Biolabelling Experiments. *Small* **2011**, *7*, 3113−3127.
(16) Lin, C.-A. J.; Sperling, R. A.; Li, J. K.; Yang, T.-Y.; Li, P.-Y.; Zanella, M.; Chang, W. H.; Parak, W. J. Design of an Amphiphilic Polymer for Nanoparticle Coating and Functionalization. *Small* **2008**, *4*, 334−341.
(17) Li, X. Shape Transformations of Bilayer Vesicles from Amphiphilic Block Copolymers: A Dissipative Particle Dynamics Simulation Study. *Soft Matter* **2013**, *9*, 11663−11670.
(18) Zhang, L.; Chan, J. M.; Gu, F. X.; Rhee, J.-W.; Wang, A. Z.; Radovic-Moreno, A. F.; Alexis, F.; Langer, R.; Farokhzad, O. C. Self-Assembled Lipid−Polymer Hybrid Nanoparticles: A Robust Drug Delivery Platform. *ACS Nano* **2008**, *2*, 1696−1702.
(19) Rodriguez-Hidalgo, M.-d.-R.; Soto-Figueroa, C.; Vicente, L. Mesoscopic Simulation of the Drug Release Mechanism on the Polymeric Vehicle P(St-Dvb) in an Acid Environment. *Soft Matter* **2011**, *7*, 8224−8230.
(20) Luo, Z.; Jiang, J. pH-Sensitive Drug Loading/Releasing in Amphiphilic Copolymer PAE−PEG: Integrating Molecular Dynamics and Dissipative Particle Dynamics Simulations. *J. Controlled Release* **2012**, *162*, 185−193.
(21) Nie, S. Y.; Lin, W. J.; Yao, N.; Guo, X. D.; Zhang, L. J. Drug Release from pH-Sensitive Polymeric Micelles with Different Drug Distributions: Insight from Coarse-Grained Simulations. *ACS Appl. Mater. Interfaces* **2014**, *6*, 17668−17678.
(22) Pogodin, S.; Baulin, V. A. Can a Carbon Nanotube Pierce through a Phospholipid Bilayer? *ACS Nano* **2010**, *4*, 5293−5300.
(23) Wong, I. Y.; Almquist, B. D.; Melosh, N. A. Dynamic Actuation Using Nano−Bio Interfaces. *Mater. Today* **2010**, *13*, 14−22.
(24) Obataya, I.; Nakamura, C.; Han, S.; Nakamura, N.; Miyake, J. Mechanical Sensing of the Penetration of Various Nanoneedles into a Living Cell Using Atomic Force Microscopy. *Biosens. Bioelectron.* **2005**, *20*, 1652−1655.
(25) Kwon, E.-Y.; Kim, Y.-T.; Kim, D.-E. Investigation of Penetration Force of Living Cell Using an Atomic Force Microscope. *J. Mech. Sci. Technol.* **2009**, *23*, 1932−1938.
(26) Vakarelski, I. U.; Brown, S. C.; Higashitani, K.; Moudgil, B. M. Penetration of Living Cell Membranes with Fortified Carbon Nanotube Tips. *Langmuir* **2007**, *23*, 10893−10896.
(27) Obataya, I.; Nakamura, C.; Han, S.; Nakamura, N.; Miyake, J. Nanoscale Operation of a Living Cell Using an Atomic Force Microscope with a Nanoneedle. *Nano Lett.* **2004**, *5*, 27−30.
(28) Xie, X.; Xu, A. M.; Angle, M. R.; Tayebi, N.; Verma, P.; Melosh, N. A. Mechanical Model of Vertical Nanowire Cell Penetration. *Nano Lett.* **2013**, *13*, 6002−6008.
(29) Groot, R. D.; Rabone, K. L. Mesoscopic Simulation of Cell Membrane Damage, Morphology Change and Rupture by Nonionic Surfactants. *Biophys. J.* **2001**, *81*, 725−736.
(30) Groot, R. D.; Warren, P. B. Dissipative Particle Dynamics: Bridging the Gap between Atomistic and Mesoscopic Simulation. *J. Chem. Phys.* **1997**, *107*, 4423.
(31) Li, X.; Liu, Y.; Wang, L.; Deng, M.; Liang, H. Fusion and Fission Pathways of Vesicles from Amphiphilic Triblock Copolymers: A Dissipative Particle Dynamics Simulation Study. *Phys. Chem. Chem. Phys.* **2009**, *11*, 4051−4059.
(32) Illya, G.; Lipowsky, R.; Shillcock, J. C. Effect of Chain Length and Asymmetry on Material Properties of Bilayer Membranes. *J. Chem. Phys.* **2005**, *122*, 244901.
(33) Plimpton, S. Fast Parallel Algorithms for Short-Range Molecular Dynamics. *J. Comput. Phys.* **1995**, *117*, 1−19.
(34) Nielsen, S. O.; Ensing, B.; Ortiz, V.; Moore, P. B.; Klein, M. L. Lipid Bilayer Perturbations around a Transmembrane Nanotube: A Coarse Grain Molecular Dynamics Study. *Biophys. J.* **2005**, *88*, 3822−3828.
(35) Venturoli, M.; Smit, B.; Sperotto, M. M. Simulation Studies of Protein-Induced Bilayer Deformations, and Lipid-Induced Protein Tilting, on a Mesoscopic Model for Lipid Bilayers with Embedded Proteins. *Biophys. J.* **2005**, *88*, 1778−1798.
(36) Izrailev, S.; Stepaniants, S.; Isralewitz, B.; Kosztin, D.; Lu, H.; Molnar, F.; Wriggers, W.; Schulten, K., Steered Molecular Dynamics. In *Computational Molecular Dynamics: Challenges, Methods, Ideas*; Deuflhard, P., Hermans, J., Leimkuhler, B., Mark, A., Reich, S., Skeel, R., Eds.; Springer: Berlin Heidelberg, Germany, 1999; Vol. *4*, pp 39−65.
(37) Song, B.; Yuan, H.; Jameson, C. J.; Murad, S. Role of Surface Ligands in Nanoparticle Permeation through a Model Membrane: A Coarse-Grained Molecular Dynamics Simulations Study. *Mol. Phys.* **2012**, *110*, 2181−2195.
(38) Ding, H. M.; Ma, Y. Q. Computer Simulation of the Role of Protein Corona in Cellular Delivery of Nanoparticles. *Biomaterials* **2014**, *35*, 8703−8710.
(39) Tong, L.; Zhao, Y.; Huff, T. B.; Hansen, M. N.; Wei, A.; Cheng, J. X. Gold Nanorods Mediate Tumor Cell Death by Compromising Membrane Integrity. *Adv. Mater.* **2007**, *19*, 3136−3141.
(40) Jiang, W.; Kim, B. Y. S.; Rutka, J. T.; ChanWarren, C. W. Nanoparticle-Mediated Cellular Response Is Size-Dependent. *Nat. Nanotechnol.* **2008**, *3*, 145−150.
(41) Nel, A.; Xia, T.; Mädler, L.; Li, N. Toxic Potential of Materials at the Nanolevel. *Science* **2006**, *311*, 622−627.
(42) De Stefano, D.; Carnuccio, R.; Maiuri, M. C. Nanomaterials Toxicity and Cell Death Modalities. *J. Drug Delivery* **2012**, *2012*, 167896.
(43) Choubey, A.; Kalia, R. K.; Malmstadt, N.; Nakano, A.; Vashishta, P. Cholesterol Translocation in a Phospholipid Membrane. *Biophys. J.* **2013**, *104*, 2429−2436.
(44) Ahmad, Z.; Shah, A.; Siddiq, M.; Kraatz, H.-B. Polymeric Micelles as Drug Delivery Vehicles. *RSC Adv.* **2014**, *4*, 17028.
(45) Nasongkla, N.; Bey, E.; Ren, J.; Ai, H.; Khemtong, C.; Guthi, J. S.; Chin, S.-F.; Sherry, A. D.; Boothman, D. A.; Gao, J. Multifunctional Polymeric Micelles as Cancer-Targeted, MRI-Ultrasensitive Drug Delivery Systems. *Nano Lett.* **2006**, *6*, 2427−2430.

DOI: 10.1021/acs.jpcb.5b00825
J. Phys. Chem. B 2015, 119, 3786−3794

(46) Miyata, K.; Christie, R. J.; Kataoka, K. Polymeric Micelles for Nano-Scale Drug Delivery. *React. Funct. Polym.* **2011**, *71*, 227−234.
(47) Wojtecki, R. J.; Meador, M. A.; Rowan, S. J. Using the Dynamic Bond to access Macroscopically Responsive Structurally Dynamic Polymers. *Nat. Mater.* **2011**, *10*, 14−27.
(48) Su, J.; Chen, F.; Cryns, V. L.; Messersmith, P. B. Catechol Polymers for pH-Responsive, Targeted Drug Delivery to Cancer Cells. *J. Am. Chem. Soc.* **2011**, *133*, 11850−11853.
(49) Schmaljohann, D. Thermo- and pH-Responsive Polymers in Drug Delivery. *Adv. Drug Delivery Rev.* **2006**, *58*, 1655−1670.
(50) Chang, B.; Sha, X.; Guo, J.; Jiao, Y.; Wang, C.; Yang, W. Thermo and pH Dual Responsive, Polymer Shell Coated, Magnetic Mesoporous Silica Nanoparticles for Controlled Drug Release. *J. Mater. Chem.* **2011**, *21*, 9239.

DOI: 10.1021/acs.jpcb.5b00825
J. Phys. Chem. B 2015, 119, 3786−3794